

Progress in hydrodynamics theory and experiments for direct-drive and fast ignition inertial confinement fusion

R Betti^{1,2,3}, K Anderson^{1,3}, T R Boehly³, T J B Collins³, R S Craxton³, J A Deletrez³, D H Edgell³, R Epstein³, V Yu Glebov³, V N Goncharov³, D R Harding³, R L Keck³, J H Kelly³, J P Knauer³, S J Loucks³, J A Marozas³, F J Marshall³, A V Maximov³, D N Maywar³, R L McCrory^{2,3}, P W McKenty³, D D Meyerhofer^{1,2,3}, J Myatt³, P B Radha³, S P Regan³, C Ren^{1,2,3}, T C Sangster³, W Seka³, S Skupsky³, A A Solodov^{1,3}, V A Smalyuk³, J M Soures³, C Stoeck³, W Theobald³, B Yaakobi³, C Zhou^{1,3}, J D Zuegel³, J A Frenje⁴, C K Li^{1,4}, R D Petrasso^{1,4} and F H Seguin⁴

¹ Fusion Science Center for Extreme States of Matter and Fast Ignition Physics, University of Rochester, 250 East River Road, Rochester, NY 14623, USA

² Departments of Mechanical Engineering, and Physics and Astronomy, University of Rochester, 250 East River Road, Rochester, NY 14623, USA

³ Laboratory for Laser Energetics, University of Rochester, 250 East River Road, Rochester, NY 14623, USA

⁴ Plasma Science and Fusion Center, Massachusetts Institute of Technology, 169 Albany Street, Cambridge MA, 02139, USA

Received 23 June 2006

Published 10 November 2006

Online at stacks.iop.org/PPCF/48/B153

Abstract

Recent advances in hydrodynamics theory and experiments at the Laboratory for Laser Energetics are described. Particular emphasis is laid on improvements in the implosion stability achieved by shaping the ablator adiabat and on the newly developed designs for fast ignition fuel assembly. The results of two-dimensional simulations and a recent set of implosion experiments on OMEGA are presented to verify the role of adiabat shaping on the hydrodynamic stability of direct-drive implosions. Adiabat shaping laser pulses are also used to implode massive capsules on a low adiabat and low implosion velocity in order to assemble high density plasmas for fast ignition. The areal densities measured in implosion experiments of such targets on OMEGA are among the highest ever recorded in a laser-driven compression experiment. Slow low-adiabat implosions of massive wetted-foam DT capsules are used in the simulations to generate the fuel assemblies for different driver energies. Such dense cores are then ignited by a fast electron beam and the resulting thermonuclear yield is used to compute the target gain. It is shown that a 200 kJ UV laser can

assemble fuel yielding about 18 MJ of energy when ignited by 15 kJ of 1–2 MeV electrons.

(Some figures in this article are in colour only in the electronic version)

1. Introduction

In direct-drive [1, 2] and fast ignition [3] inertial confinement fusion, a cryogenic shell of deuterium and tritium (DT) filled with DT gas is accelerated inwards by direct laser irradiation (direct-drive). If the thermonuclear fuel is ignited and a burn wave propagates through the dense core, the fusion energy produced can greatly exceed the laser energy used to drive the target. The energy gain G is defined as the ratio between the thermonuclear energy yield and the laser energy on target. The gain is directly related to the capsule implosion velocity, $G = (1/V_1^2)\eta_h\theta E_f/m_i$ (see for example [4]) where V_1 is the implosion velocity, $\eta_h = E_K/E_L$ is the hydrodynamic efficiency representing the ratio between the shell kinetic energy and the laser energy on target, $E_f = 17.6$ MeV is the energy of the fusion products for a DT fusion reaction and $m_i = 2.5m_H$ is the average ion mass. The function θ represents the fraction of burned fuel depending on the fuel areal density $\rho R \equiv \int_0^R \rho dr$. The function $\theta = \theta(\rho R)$ is commonly approximated [1] by $\theta \simeq (1 + 7/\rho R)^{-1}$ where ρR is given in g cm^{-2} . If the energy is kept constant, higher implosion velocities require lower target masses and the effect on the ρR of a lower mass balances the effect of higher velocities thus making ρR approximately independent of velocity. A simple expression for the areal density is derived in [4] where an analytic scaling is benchmarked against a numerical fit leading to

$$(\rho R)_{\max} \approx \frac{1.2}{\alpha_{\text{inn}}^{0.55}} \left(\frac{E_L(\text{kJ})}{100} \right)^{0.33}, \quad (1)$$

where α_{inn} is the adiabat of the inner portion of the shell and ρR is in g cm^{-2} . In inertial fusion hydrodynamics, the adiabat is usually referred to as the ratio of the pressure to the Fermi pressure of a fully degenerate electron gas and, for a DT plasma, it can be conveniently written as

$$\alpha \equiv \frac{P(\text{Mb})}{2.2\rho(\text{g/cc})^{5/3}}, \quad (2)$$

where P is the pressure in megabars and ρ is the density in g/cc . The adiabat is a measure of the entropy and is typically set by the shocks propagating through the target. The inner adiabat enters the areal density because the outer portion of the shell is ablated during the implosion and only the inner portion is left to form the dense stagnating core. Equation (1) shows that for a given laser energy, higher areal densities require lower inner adiabats.

The hydrodynamic efficiency depends mainly on the shell velocity [4] and, for a UV laser with $\lambda_L = 0.35 \mu\text{m}$, it scales approximately as $\eta_h^{\text{fit}} \sim V_1^{0.75} I_L^{-0.25}$ where I_L is the laser intensity. Substituting the efficiency into the gain formula and using a set of one-dimensional simulations to determine the proportionality constant yields a thermonuclear gain inversely proportional to the implosion velocity

$$G \approx \frac{73}{I_{15}^{0.25}} \left(\frac{3 \times 10^7}{V_1} \right)^{1.25} \left(\frac{\theta(\rho R)}{0.2} \right), \quad (3)$$

where V_1 is in cm s^{-1} and I_{15} is the laser intensity in units of 10^{15} W/cm^2 . Equation (3) shows that for the same implosion velocity, higher gains can be achieved by increasing the driver energy and by reducing the shell adiabat thus increasing the maximum ρR . For a fixed driver energy, higher gains can only be achieved through lower implosion velocities (and greater fuel mass) and lower adiabats.

In conventional hot-spot ignition ICF, a compressed shell of thermonuclear fuel is ignited from a low-density central hot spot. For ignition to occur, the alpha particle self-heating of the hot spot must exceed all the energy losses. Since the hot-spot temperature is mostly dependent on the shell velocity, the energy required for ignition decreases with the shell velocity [5] ($E_{\text{ign}} \sim \alpha_{\text{inn}}^{1.8}/V_i^6$). The main problem with high velocity implosions is that they are highly unstable during the acceleration phase and the shell breaks up before stagnating. The growth rate of the acceleration phase RT instability for a directly driven DT capsule can be written [6] as $\gamma_{\text{RT}} = 0.94\sqrt{kg} - 2.7kV_a$ where k is the mode wave number, g is the acceleration and V_a is the ablation velocity. The RT growth factor is $\exp(\gamma t)$ and $\gamma t = N_e$ is the number of e-foldings. Using the growth rate formula, one can rewrite the number of e-foldings as

$$N_e = 1.33\sqrt{(k\Delta)\mu\langle\text{IFAR}\rangle} - 5.4(k\Delta)\mu(V_a/V_i), \quad (4)$$

where $\mu = D/R$ is the ratio between the distance travelled by the shell D and the target radius R , $\langle\text{IFAR}\rangle = \langle R/\Delta \rangle$ is the time average in-flight aspect ratio and Δ is the in-flight thickness. Since the maximum aspect ratio is proportional to the square of the Mach number, it can be related to the implosion velocity and the shell adiabat through the simple relation

$$\text{IFAR}_{\text{max}} \simeq \frac{51}{\langle\alpha_{\text{if}}\rangle^{0.6}} \left(\frac{V_i(\text{cm s}^{-1})}{3 \times 10^7} \right)^2 \frac{1}{I_{15}^{4/15}}, \quad (5)$$

where $\langle\alpha\rangle$ represents a spatial average of the in-flight shell adiabat. By dividing the shell into an outer portion by the ablation front and an inner portion by the inner shell surface, the average adiabat is a value between α_{inn} and α_{outer} , assuming that the adiabat profile is monotonic. Conventional implosions are designed with a flat adiabat profile leading to $\alpha_{\text{inn}} \approx \alpha_{\text{out}}$. Typically, the shell aspect ratio varies from $\text{IFAR} = \text{IFAR}_{\text{max}} \gg 1$ at the beginning of the acceleration phase to $\text{IFAR} \sim 1$ at the end, so an averaged value $\langle\text{IFAR}\rangle \simeq 0.6 \times \text{IFAR}_{\text{max}}$ is typically a good approximation. The energy required for hot-spot ignition scales approximately as

$$E_{\text{ign}} \sim \left(\frac{1}{\text{IFAR}} \right)^3 \left(\frac{\alpha_{\text{inn}}}{\langle\alpha\rangle} \right)^{1.8} \quad (6)$$

indicating that low IFAR implosions require large laser energies for ignition. Since the mode numbers causing shell break-up are those with $k\Delta \approx 1$, the number of e-foldings for those modes can be rewritten upon substitution of (5) into (4) and by using the simple formula [2] for the ablation velocity $V_a \simeq 1.15 \times 10^5 \alpha_{\text{out}}^{3/5} I_{15}^{-1/15} \text{ cm s}^{-1}$ for a $0.35 \mu\text{m}$ light. Here α_{out} is the adiabat on the outer shell surface where laser ablation takes place and the Rayleigh-Taylor instability develops. A straightforward manipulation yields a number of e-foldings for $k\Delta = 1$ proportional to the implosion velocity

$$N_e = \frac{V_i}{3 \times 10^7} \left[\frac{6.2}{\langle\alpha\rangle^{0.3} I_{15}^{2/15}} - \frac{0.45}{I_{15}^{1/3}} \left(\frac{\alpha_{\text{out}}}{\langle\alpha\rangle} \right)^{0.6} \right], \quad (7)$$

where $\mu \simeq 0.7$ has been used. Two important conclusions can be extracted from equation (7): the first is that high implosion velocities lead to large growth factors; the second is that increasing the outer surface adiabat (i.e. larger $\langle\alpha\rangle$ and $\alpha_{\text{out}}/\langle\alpha\rangle$) leads to improved stability. Notice also that for a fixed IFAR, a large α_{out} improves the ignition condition as shown in equation (6). Another advantage of increasing α_{out} is that for the same stability characteristics, the areal density can be increased by decreasing α_{inn} , thus improving the target gain.

In direct-drive fast ignition [3], the energy gains can still be determined through equation (3). Different from conventional ICF, the high density and high areal-density assembly of thermonuclear fuel is ignited by the external heating of a small volume of the dense fuel.

The external heating is provided by the fast electrons accelerated by the interaction of an ultra-intense petawatt laser pulse with either the coronal plasmas or a solid target. For inertial fusion energy applications, the thermonuclear gain must be greater than 100 and the areal density must be at least $2.5\text{--}3\text{ g cm}^{-2}$. Since the areal density is approximately independent of the implosion velocity, the highest gains of fast ignited targets are achieved for low velocity implosions that carry more mass for the same laser energy. In order to achieve the required core density [7] of about 300 g cm^{-3} , fast ignition implosions need to be driven on a very low inner adiabat [4]. As shown in [4], a convenient and hydrodynamically stable method to design slow low-adiabat implosions for fast ignition is by shaping the adiabat inside the shell [8–11].

Based on the considerations above, shaping the adiabat inside the imploding shell is a convenient path to follow in order to optimize the implosion stability without compromising the energy gain in both conventional and fast ignition inertial fusion.

It has been shown by Goncharov *et al* [8], and Anderson and Betti [9–11] that shaping the adiabat can be easily accomplished by adding a laser intensity spike at the beginning of the laser pulse and by appropriately redesigning the main laser pulse that follows.

Target designs for direct-drive and fast ignition as well as recent experiments on the OMEGA laser are described in this paper.

2. Adiabatic shaping: theory and experiments

Two different techniques have been proposed to shape the adiabat in the ablator: (1) adiabat shaping via a decaying shock (DS) [8, 9] and (2) adiabat shaping by relaxation (RX) [10, 11]. Shaping by a DS was first introduced in [8] and requires a very strong prepulse aimed at launching a strong shock. Such a strong shock decays inside the shell, shortly after the prepulse is turned off, with a low intensity foot of the main pulse following. The DS creates a monotonically-decreasing adiabat profile that follows a power law of the mass coordinate

$$\alpha_{\text{DS}} \simeq \alpha_{\text{inn}} \left(\frac{m_{\text{shell}}}{m} \right)^{\delta_{\text{DS}}}, \quad (8)$$

where m is the mass calculated from the outer surface, m_{shell} is the total shell mass and α_{inn} is the adiabat on the shell inner surface. The value of δ_{DS} , calculated in [9], is approximately independent of the prepulse characteristics. Without accounting for the effect of mass ablation, δ_{DS} is about 1.3. If mass ablation is included, δ_{DS} varies between 1.06 and 1.13 depending on the prepulse duration. Two-dimensional simulations [8, 12] of OMEGA-size capsule implosions have confirmed that DS-shaped targets exhibit significantly reduced Rayleigh–Taylor growth on the ablation surface during the acceleration phase with respect to the flat adiabat ones. Comparisons between flat and shaped adiabat targets are typically carried out by designing the flat and shaped adiabat pulses leading to identical adiabats on the inner shell-surface.

A different technique aimed at shaping the adiabat is the so-called shaping by relaxation (or RX shaping) first introduced in [10]. The RX technique uses a less energetic pressure prepulse than the DS technique. The RX prepulse is turned off before the prepulse shock reaches the shell's inner surface. Since the prepulse is followed by a complete power shut off, the outer portion of the shell expands outwards generating a relaxed density profile while the prepulse shock travels inside the shell. The prepulse shock is not intended to greatly change the shell adiabat even though it may cause a significant adiabat modification. The main adiabat shaping occurs later in time when the foot of the main pulse starts and a strong shock travels up the relaxed density profile. The main shock first encounters the low-density portion of the relaxed profile setting it on a very high adiabat. The adiabat develops a monotonically decreasing profile as a result of the increasing pre-shock density. Two-dimensional simulations [10, 12] of

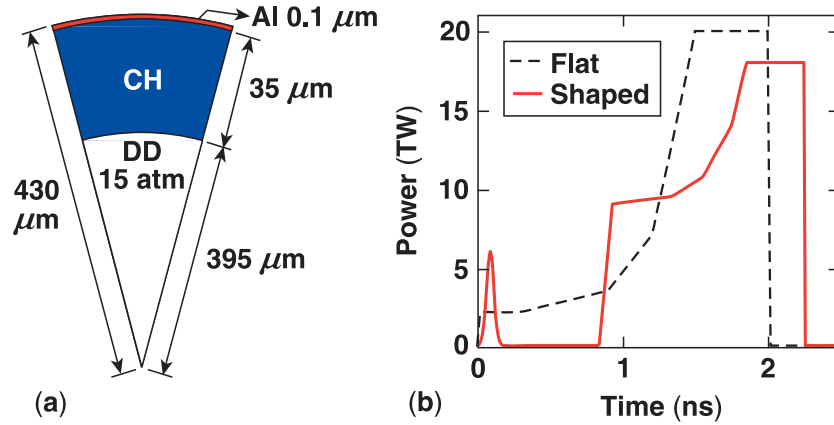


Figure 1. Target (a) and laser pulse shapes (b) used in adiabat shaping experiments on the OMEGA laser. The pulse shapes are for the flat (dashed black) and shaped (solid red) adiabat implosions.

OMEGA-size capsule implosions have confirmed that RX-shaped targets exhibit significantly reduced Rayleigh–Taylor growth on the ablation surface during the acceleration phase with respect to the flat adiabat ones. Similarly to the DS shaping, the RX adiabat profile can be approximated with a power law [11] of the mass coordinate

$$\alpha_{\text{RX}} \simeq \alpha_{\text{inn}} \left(\frac{m_{\text{shell}}}{m} \right)^{\delta_{\text{RX}}}, \quad (9)$$

where δ_{RX} can be tailored between a minimum of zero (i.e. no shaping) and a maximum value of 2.4. This upper bound, which is well above the DS value, can only be achieved for weak prepulses (either low pressure or short duration prepulses) and by neglecting the effects of mass ablation. For realistic prepulses and including the effect of ablation, the maximum RX power index is reduced to values in the range 1.6–1.8 which is still significantly larger than the 1.1 of the DS. The steeper RX adiabat profile leads to greater values of the outer surface adiabat with respect to the DS adiabat shaping, thus leading to larger ablation velocities and more effective ablative stabilization. Since the seeds of the RT are as important as the growth rates in ICF implosions, the large intensity spike used in the DS shaping has the important advantage of significantly reducing the level of laser imprinting on target [13]. The smaller spike of the RX shaping may also reduce imprinting [12, 14] but at a lower level than the DS spike.

The adiabat shaping concept has been tested [15] on the OMEGA laser system by imploding plastic (CH) shells. Implosions of 35 μm thick, 430 μm radius CH shells have been designed [12] with and without adiabat shaping. The flat and shaped adiabat pulse shapes and the CH target are shown in figure 1. The flat adiabat design leads to an adiabat shape approximately uniform and equal to about 3. The shaped adiabat profile is about 3 on the inner surface and about 12 on the ablation (outer) surface. At the end of the laser pulse, the two adiabat profiles are similar thus leading to approximately the same one-dimensional performance. Figure 2 shows the plot in the r, θ plane of the outer (ablation) and inner shell surfaces of the target in figure 1 obtained [12] from a two-dimensional multimode simulation with modes $l = 2$ –200 using the code DRACO [16]. The plots are taken 130 ps after the end of the laser pulse. For the sake of clarity, the plot is restricted to a cone angle of 30°. The initial perturbations are seeded by the laser nonuniformities typical of the OMEGA laser

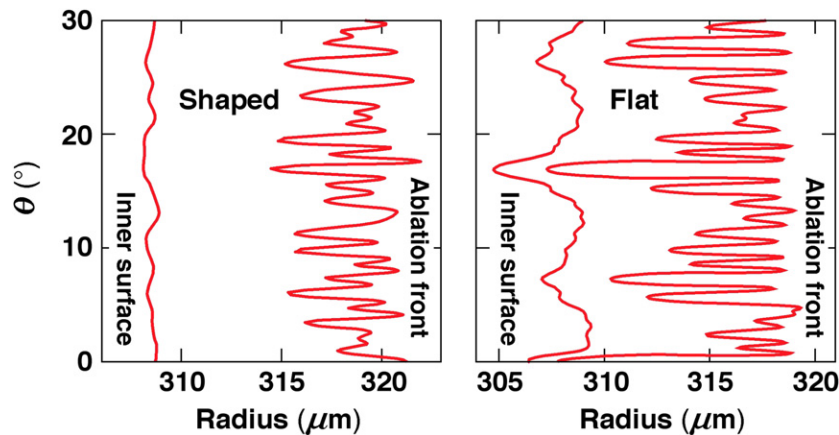


Figure 2. Outer and inner surfaces of the shaped (left) and flat (right) adiabat implosion of the CH shell in figure 1. The surfaces are shown in a (r, θ) plot and 130 ps after laser shut-off.

system with 1 THz SSD (smoothing by spectral dispersion [17]). Figure 2 clearly shows that the ablation (outer) surface is much less distorted in the shaped adiabat implosions with respect to the flat adiabat. The σ_{RMS} of the perturbation is $2.90 \mu\text{m}$ on the outer surface and $1.22 \mu\text{m}$ on the inner surface for the flat adiabat. For the shaped adiabat, the σ_{RMS} is significantly less: $1.73 \mu\text{m}$ on the outer and $0.34 \mu\text{m}$ on the inner, thus confirming that adiabat shaping greatly improves the target stability. Implosion experiments [15] with $35 \mu\text{m}$ shells filled with 15 atm D_2 gas (figure 1) have been carried out on the OMEGA laser system. The experimental pulse shapes are very close to the theoretical ones shown in figure 1. The total experimental laser energy was $E_L = 17.3 \pm 0.2 \text{ kJ}$. In order to better identify the effect of adiabat shaping, two sets of implosions [15] with and without SSD laser smoothing are compared. The total neutron yield is measured and compared between shaped and flat adiabat pulses. Figure 3 shows the neutron yield with and without SSD and flat versus shaped adiabat. Adiabat shaped implosions show significantly better performance with respect to the flat adiabat ones, with the relative neutron yield increasing by 23% with SSD on and by 136% with SSD off. It is important to note that the neutron yields of the flat adiabat implosions are strongly dependent on the laser smoothing. Since SSD is particularly efficient in reducing the short wavelength laser nonuniformities, one can conclude that adiabat shaped implosions are not strongly affected by such modes even when the initial imprinted nonuniformities are large as in the case with SSD off. On the contrary, flat adiabat implosions are strongly affected by the laser smoothing as shown by the sharp decrease in neutron yields when SSD is off.

In conclusion, multimode simulations (figure 2) and implosion experiments (figure 3) indicate that shaping the adiabat through a laser intensity spike significantly improve the target stability by reducing the growth of surface nonuniformities thus leading to an improved performance.

3. Fast ignition fuel assembly and energy gains

Similar considerations used in the design of direct-drive implosions can be used to design capsules and laser pulses to optimize the fuel assembly [4] for fast ignition [3]. Hydrodynamic simulations and experiments can then be used to characterize the compressed

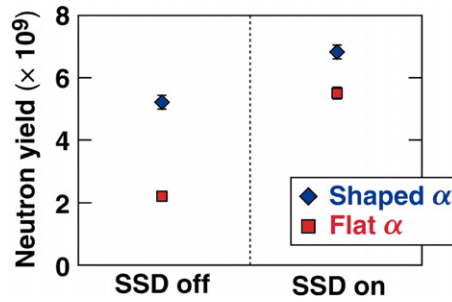


Figure 3. Experimental neutron yields for flat and shaped adiabat implosions, with and without SSD.

core. Thermonuclear gains can be obtained from numerical simulations of the interaction of an energetic electron (or proton) beam and the compressed core.

The first step is the design of optimized implosions [4] for fast ignition. Since central high temperatures are not important, if not detrimental, to fast ignition, the implosions can be slow [4] since the temperature is proportional to the implosion velocity. For the same driver energy, slow implosions require massive shells leading to large fuel masses and therefore large gains. However, low velocities also lead to low densities [4] since the density is directly proportional to the implosion velocity. Since the density is also inversely proportional [4] to the inner shell adiabat, one can design a fast ignition implosion of a massive shell driven on a low implosion velocity as long as the inner adiabat is kept low enough to compensate for the low V_I and still produce the high densities required for ignition. Therefore, optimized fast ignition targets are massive shells of DT fuel (preferably wetted-foams) driven on a very low inner adiabat. Another advantage of keeping the adiabat low is that the areal density increases for lower adiabats leading to a higher burn fraction and higher gains. Laser pulses for very low-adiabat ($\alpha < 1$) implosions are typically difficult to design and to implement since, at first, the laser intensity needs to be kept very low to drive a relatively weak shock that does not fully ionize the target (thus the adiabat values less than unity). After launching the first shock, the laser intensity needs to be slowly increased until it reaches a flat top value that can be as high as hundreds of times the initial value. A contrast ratio greater than 100–150 (intensity ratio between the flat top and the foot of the laser pulse) is probably hard to achieve with current laser technology. However, using a RX-type adiabat shaping pulse (see section 2), the main pulse can be designed with a contrast ratio typically half the value of a standard continuous pulse without initial intensity spike. Therefore, adiabat shaping has been used in [4] to design the pulse shapes to implode the low-adiabat fast ignition targets. In fast ignition, the use of adiabat shaping pulses is mostly motivated by the technological reasons connected to the laser pulse feasibility rather than hydrodynamic stability. As indicated in [4], the optimized fuel assembly for fast ignition can be obtained by driving massive shells of wetted-foams on a velocity of about $1.7 \times 10^7 \text{ cm s}^{-1}$ and inner surface adiabat of $\alpha_{\text{inner}} \approx 0.7$. Such implosions lead to high areal densities and high densities in the range $300\text{--}500 \text{ g cm}^{-3}$.

Having defined the optimized ignition targets and the laser pulse shapes, the gain calculation can be easily carried out. The maximum gain $G_M = E_F/E_c$ is defined as the ratio between the thermonuclear energy E_F and the compression laser energy on target E_c . The total gain $G_T = E_F/E_T$ is the ratio between the thermonuclear energy and the total laser energy on target including the petawatt laser energy $E_T = E_c + E_{\text{pw}}$. Using the conversion efficiency [18] η_{pw} of the petawatt laser energy into collimated fast particles, the petawatt laser energy on target

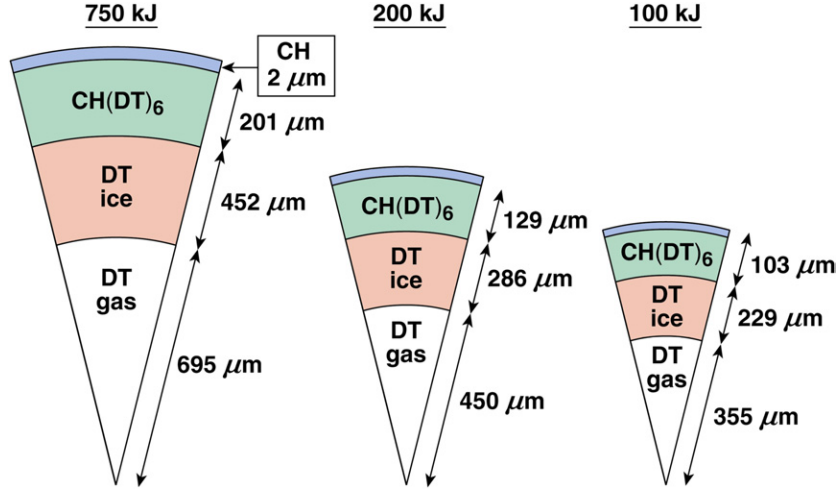


Figure 4. Wetted-foam fast ignition targets designed for 100, 200 and 750 kJ direct-drive implosions. The driver is a UV laser with $\lambda_L = 0.35 \mu\text{m}$.

is $E_{pw} = E_{fp}/\eta_{pw}$ where E_{fp} represents the minimum energy [7] required for ignition E_{ig}^{\min} . The complications related to the fast electron generation and transport are included into η_{pw} . The scope is limited to the target gain calculations parametrized with η_{pw} without addressing the issues related to the fast electrons generation and transport. The maximum gain G_M is nothing more than the general relation given in equation (3) and valid for both fast ignition and conventional ignition as long as ignition occurs and a burn wave propagates through the dense core. Using the values [4] of $V_i = 1.7 \times 10^7 \text{ cm s}^{-1}$ and $\alpha_{\text{inner}} = 0.7$ for the implosion velocity leads to a maximum gain formula that only depends on the laser energy

$$G_M \approx \frac{743(1 - E_{\text{cut}}/E_c)^\mu}{1 + 21/[\xi E_c^{0.33}]}, \quad (10)$$

where E_c is in kilojoule, and ξ represents the fraction of the maximum total areal density available for the burn to be used in $\theta(\rho R)$ [$\rho R = \xi(\rho R)_{\text{max}}$]. The *ad hoc* term $(1 - E_{\text{cut}}/E_c)^\mu$ has been introduced to account for the yield deterioration of small targets where the e-beam size is of the order of the compressed core size occurring for $E_c \sim E_{\text{cut}} \approx 40 \text{ kJ}$. The factors μ and ξ are of order unity and are determined by a numerical fit. It is important to emphasize that slow implosions with $V_i < 2 \times 10^7 \text{ cm s}^{-1}$ are not significantly affected by the RT instability. For such low implosion velocities, the in-flight aspect ratio is very low and the hydrodynamic instabilities have negligible effects on the implosion performance.

This allows the use of the one-dimensional code LILAC [19] to simulate the generation of the dense core of the fast ignition fuel assembly (in the absence of a cone). In order to simulate the burn phase of the fast ignited capsules, we start from the one-dimensional fuel assembly and simulate the ignition by a collimated electron beam and subsequent burn with the two-dimensional two-fluids hydro-code DRACO [16]. The latter has been modified to include the electron beam energy deposition into the dense fuel. The fast electron energy (1–3 MeV), beam radius (15–25 μm) and pulse length (5–15 ps) are varied to determine the minimum electron beam ignition energy of 15 kJ. As long as fast ignition is triggered, the thermonuclear energy yield is approximately independent of the electron beam characteristics. We have performed burn simulations of several fuel assemblies characterized by the implosion parameters mentioned above. The targets used in the simulations (figure 4 shows three of them)

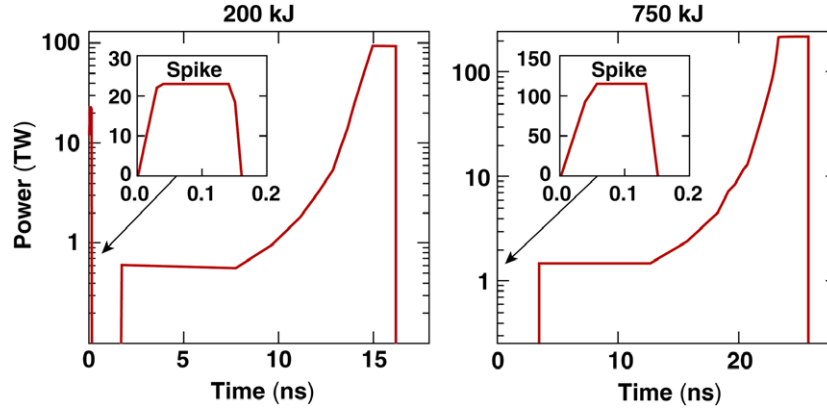


Figure 5. Adiabatic shaping UV laser pulses ($\lambda_L = 0.35 \mu\text{m}$) for the 200 and 750 kJ targets.

are massive wetted-foam targets with initial aspect ratio of about 2 (outer radius/thickness) driven by UV laser energies from 50 kJ to 2 MJ and $I_{15} \simeq 1$.

The RX laser pulses for the 200 and 750 kJ targets are shown in figure 5 with the main pulse length varying from 15 ns for the 200 kJ target to 22 ns for the 750 kJ target. In all cases, the fast electrons are injected after the time of peak areal density when the average density of the compressed core is about $300\text{--}400 \text{ g cm}^{-3}$ and the ρR of the compressed shell is close to its maximum value. The neutron yields for the 100 kJ, 200 kJ and 750 kJ assemblies are 2.0×10^{18} , 6.4×10^{18} and 4.2×10^{19} and the thermonuclear energy yields are 5.6, 18 and 118 MJ, respectively. The results of these simulations are used to determine $\xi \approx 0.7$ and $\mu \approx 1.1$ leading to a maximum gain

$$G_M \approx \frac{743 I_{15}^{-0.09} (0.35/\lambda_L)^{0.66} (1 - E_{\text{cut}}/E_c)^{1.1}}{1 + 30(\lambda_L/0.35)^{0.25}/E_c^{0.33}}, \quad (11)$$

where E_c is in kilojoules and $E_{\text{cut}} \approx 40 \text{ kJ}$. The gain formula in equation (11) has been generalized to include the laser wavelength and intensity dependence. The gain curve representing the maximum gain, i.e. the ratio between the energy yield and the compression driver energy for $\lambda_L = 0.35 \mu\text{m}$ and $I_{15} = 1$ is shown in figure 6(a) where the result of the burn simulation is superimposed on the gain curve from equation (11). Notice that even a modest size UV laser driver with an energy of 200 kJ can produce a fuel assembly yielding a maximum gain close to 90. Using $E_{\text{ig}}^{\text{min}} \simeq 15 \text{ kJ}$ and setting the petawatt laser energy equal to $E_{\text{pw}} = E_{\text{ig}}^{\text{min}}/\eta_{\text{pw}}$, the total target gain can be plotted for different values of the conversion efficiency η_{pw} . Figure 6(b) shows the target gain G_T for $\eta_{\text{pw}} = 0.1, 0.2$ and 0.3 . Even in the case of only 10% efficiency, the target gain from a 200 kJ fuel assembly is still remarkably high ($G_T \approx 70$), indicating that fast ignition can achieve significant gains with relatively small drivers. However, achieving the ignition requirement of a 15 kJ collimated beam still remains a very challenging task.

Achieving high gains in fast ignition is possible only if the fuel can be assembled through low-adiabat and low-velocity implosions leading to large fuel masses compressed to densities of hundreds of g cm^{-3} . A series of experiments [20] have been carried out on the OMEGA laser to optimize the fuel assembly for fast ignition through low-velocity, low-adiabat implosions. Thick CH shells ($40 \mu\text{m}$ thick and $430 \mu\text{m}$ in outer radius) have been driven by a RX laser pulse. The capsules, shown in figure 7(b), were filled with D_2 and DHe_3 and driven by the 20 kJ laser pulse shown in figure 7(a). One-dimensional simulations of the implosion indicate

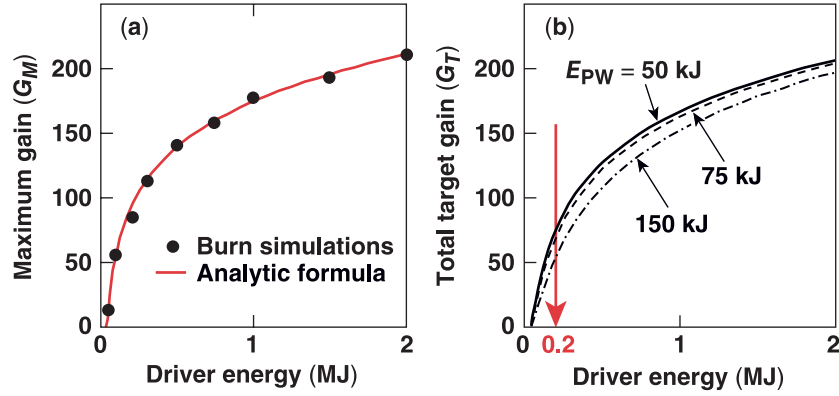


Figure 6. (a) Maximum gain (fusion energy/compression driver energy) versus compression driver energy. The dots are the results of the burn simulations while the curve is from equation (11). (b) Total target gain (fusion energy/total laser energy on target) versus compression driver energy for $E_{pw} = 50$ kJ ($\eta_{pw} = 0.3$, solid), $E_{pw} = 75$ kJ ($\eta_{pw} = 0.2$, dashed) and $E_{pw} = 150$ kJ ($\eta_{pw} = 0.1$, dashed-dotted).

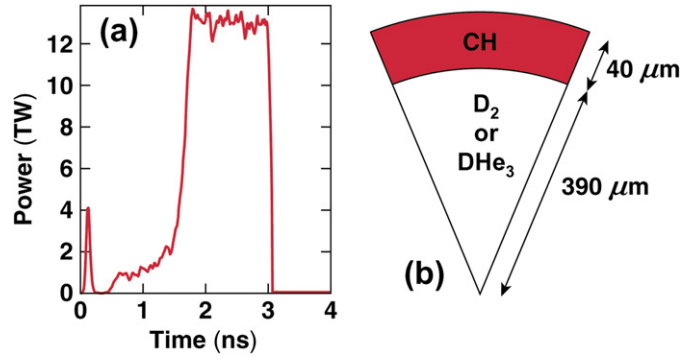


Figure 7. A 40 μm CH capsule (b) and the 20 kJ laser pulse (a) driving the shell on $\alpha_{\text{inn}} \approx 1.3$ and implosion velocity $V_i \approx 2 \times 10^7$ cm s^{-1} .

that the implosion velocity was about 2×10^7 cm s^{-1} and the inner adiabat was $\alpha_{\text{inn}} \approx 1.3$. The spectrum of the protons from the primary D+He₃ fusion reactions and those from the secondary D+He₃ reactions were measured for the DHe₃ fills and D₂ fills, respectively.

The energy downshift of the proton spectra is correlated [21] with the shell areal density ρR . The ρR inferred from the proton spectroscopy is a time average value over the proton production rate and has been compared with the simulated ρR averaged over the experimentally measured neutron rate from the D+D fusion reactions. Averaging the simulated ρR over the proton rate was not possible due to the low yields of the D+He₃ reactions. Preliminary analyses of the experimental results show that the experimental proton average and theoretical neutron average areal densities are in very good agreement and equal to 0.14 g cm^{-2} . Such ρR s were among the largest areal densities (if not the largest) ever assembled in a laser-driven implosion. It is important to emphasize that the areal density peaks a few hundred picoseconds after the peak of the fusion rate and therefore it cannot be directly measured by nuclear diagnostics relying on fusion yields. Therefore, the maximum value of the areal density can only be inferred from the one-dimensional simulations indicating a peak $\rho R \approx 0.28$ g cm^{-2} . Therefore, the assemblies produced in the OMEGA CH-shell implosions should have reached an areal density

through the entire core (i.e. $2\rho R$) of about 0.56 g cm^{-2} sufficient to slow down $\sim 2\text{ MeV}$ electrons.

4. Conclusions

A series of experiments and two-dimensional simulations of plastic shell implosions have been carried out to investigate the effect of adiabat shaping on the hydrodynamic stability of direct-drive implosions. The CH capsules were imploded with a 17 kJ laser pulse driving the shell on an adiabat $\alpha \approx 3$. Two sets of pulses have been used: a standard continuous pulse designed to keep the adiabat profile flat inside the shell and a picket pulse with an intensity spike designed to shape the adiabat. The shaped adiabat implosions showed a significant improvement in performance with respect to the flat adiabat ones. Without laser smoothing, the neutron yield from shaped adiabat implosions was about 140% higher than in flat adiabat ones. The same type of laser pulses has been used to implode very thick plastic shells on a very low adiabat and low velocity in order to generate massive assemblies of dense plasma optimal for fast ignition. Low-velocity, low-adiabat implosions of massive CH shells on the OMEGA laser system have been used to study the large areal-density assemblies. The measured ρR s are in good agreement with one-dimensional simulation results averaged over the neutron rate from D+D fusion reactions. The maximum ρR of such implosions occurs after the peak of the fusion rate and is inferred from the simulations indicating peak values close to 0.3 g cm^{-2} .

Acknowledgments

This work has been supported by the US Department of Energy under Cooperative Agreement ER54789 (Fusion Science Center) and DE-FC03-92SF19460 (Office of Inertial Confinement Fusion).

References

- [1] Atzeni S and Meyer-ter-Vehn J 2004 *The Physics of Inertial Fusion* (Oxford: Clarendon Press)
- [2] Lindl J D 1998 *Inertial Confinement Fusion* (New York: Springer)
- [3] Tabak M *et al* 1994 *Phys. Plasmas* **1** 1626
- [4] Betti R and Zhou C 2005 *Phys. Plasmas* **12** 110702
- [5] Herrmann M C, Tabak M and Lindl J D 2001 *Nucl. Fusion* **41** 99
Kemp A, Meyer-ter-Vehn J and Atzeni S 2001 *Phys. Rev. Lett.* **86** 3336
Betti R *et al* 2002 *Phys. Plasmas* **9** 2277
- [6] Betti R *et al* 1998 *Phys. Plasmas* **5** 1446
Takabe H *et al* 1985 *Phys. Fluids* **28** 3676
- [7] Atzeni S 1999 *Phys. Plasmas* **6** 3316
- [8] Goncharov V *et al* 2003 *Phys. Plasmas* **10** 1906
- [9] Anderson K and Betti R 2003 *Phys. Plasmas* **10** 4448
- [10] Anderson K and Betti R 2004 *Phys. Plasmas* **11** 5
- [11] Betti R *et al* 2005 *Phys. Plasmas* **12** 042703
- [12] Anderson K 2006 *PhD Thesis* University of Rochester, Rochester NY, USA
- [13] Collins T J B and Skupsky S 2002 *Phys. Plasmas* **9** 275
- [14] Metzler N, Velikovich A L, Schmitt A J and Gardner J H 2002 *Phys. Plasmas* **9** 5050
- [15] Knauer J P *et al* 2005 *Phys. Plasmas* **12** 056306
- [16] Radha P B *et al* 2005 *Phys. Plasmas* **12** 032702
- [17] Skupsky S, Short R W, Kessler T, Craxton R S, Letzring S and Soures J M 1989 *J. Appl. Phys.* **66** 3456
- [18] Tabak M *et al* 2005 *Phys. Plasmas* **12** 057305
- [19] Richardson M C 1986 *Laser Interaction and Related Plasma Phenomena* **7** 421 (New York: Plenum)
- [20] Theobald W and Zhou C 2006 private communications
- [21] Petrasso R D *et al* 2003 *Phys. Rev. Lett.* **90** 135002